

## DYNAMIC PROPERTIES OF REINFORCED CONCRETE PIERS

H. Mutsuyoshi (I)

A. Machida (II)

Presenting Author: H. Mutsuyoshi

### SUMMARY

Small scale reinforced concrete(R.C.) specimens, which have similar cross sectional characteristics to ordinary R.C. piers of a single column type, were tested under static cyclic loading, dynamic loading and dynamic base motion. The differences between the mechanical properties of R.C. piers under dynamic loading and static loading were clarified.

The load-displacement characteristics under monotonous dynamic loading are considerably influenced by the loading rates, whereas remarkable differences due to the loading rate were hardly recognized between the load-displacement characteristics under static cyclic loading and dynamic cyclic loading.

### INTRODUCTION

The properties of R.C structures subjected to earthquakes have been studied mainly for building structures, but studies of R.C. bridge piers of a single column type subjected to severe earthquakes have been conducted less frequently. In general, cross sectional characteristics, such as the main reinforcement ratio and the shear reinforcement ratio, the magnitude of the axial forces of R.C. piers of a single column type are widely different from those of R.C. columns of building structures. Therefore, it is necessary to clarify characteristics of R.C. piers subjected to dynamic loading independently of R.C. columns of building structures.

Dynamic analyses and earthquake resistant design for R.C. structures commonly have been conducted on the basis of the assumption that characteristics under dynamic loading are equal to those under static loading. It has hardly been clarified, however, whether fundamental properties of R.C. structures under dynamic loading are equal to those under static loading.

The objective of this paper is to make clear the differences between the mechanical properties of R.C. piers under dynamic loading and static loading.

### TEST PROGRAM

#### Dynamic Loading Test

The cross section of all the specimens was 10x15 cm, and the height was 56 cm, as shown in Fig 1. Table 1 describes the properties of the specimens. Two kinds of the loading methods were used in the dynamic tests. One was monotonous dynamic loads in one direction and another was dynamic cyclic loads operated with sine waves. Dynamic loads were applied at the top of the specimen and the loading rates of 0.1, 10 and 100 (cm/s) were adopted as the

- 
- (I) Research Associate of Construction Engineering, Saitama University
  - (II) Associate Professor of Construction Engineering, Saitama University,  
Saitama, Japan

dynamic loads. The reason why the loading rates described above were used is as follows; the loading rate of 0.1 cm/s corresponds to that of the static tests conducted in general, and the loading rate of 100 cm/s was determined based on the maximum response velocity and strain rate which can occur in actual R.C. piers subjected to severe earthquakes. The displacement amplitude at the top of the specimen and the frequency for the dynamic cyclic loads were determined so that the displacement rates could satisfy the loading rates mentioned previously (see Table 3). The displacement amplitudes were always equal to the integral multiples of the yield displacement, and the number of the repetition at a certain displacement was 10 cycles. The loading program is shown in Fig.2.

When the dynamic cyclic load is applied at the top of the specimen, the inertia force, which is given as the product of the acceleration in the loading direction and mass of the equipment fixed at the top of the specimen (including mass of the equipment fixed in the exterior side of load cell at the tip of the actuator) and the column of the specimen, is produced horizontally. In addition to this horizontal inertia force, the vertical inertia force is also produced because the actuator moves up and down in a vertical line, so that the vertical inertia force is applied to the specimen as an eccentric load. Such an eccentric load in the loading rate of 100 cm/s is very large and influences the behaviors of the specimen significantly. Therefore, the actuator was fixed and the device which is able to rotate and move up and down was installed at the tip of the actuator in order that the vertical inertia force should not be produced. The loading system for the dynamic loading tests is indicated in Fig.3.

#### Shaking Table Test and Static Cyclic Test

The specimens used in the shaking table tests were the same specimens as shown in Fig.1 except that the height of the column was 60 cm. Table 2 describes the properties of the test specimens. Six specimens were tested statically, and eight specimens were tested dynamically. In every test, the weight of 833 kgf was installed at the top of the specimen and this weight is able to rotate around its central axis so that the moment of inertia is eliminated. The axial stress caused by the weight was  $5.5 \text{ kgf/cm}^2$ .

In the shaking table tests, the specimen was fixed on the shaking table at the base, and the shaking table was operated with sine waves. The frequency of the shaking table was decreased stepwise according to the measured displacement at the top of the specimen in order that the frequency of the shaking table should be nearly equal to the natural frequency of the specimen, which was obtained from load-displacement characteristics, as shown in Fig.4. That is, the specimens were tested dynamically in a state of the near resonance. The shaking table test was carried out continuously up to failure for each of the specimens.

In the static tests, a specimen was fixed at the base, and the reversal horizontal force, which produced a constant horizontal displacement amplitude, was applied cyclically. The number of the repetition of static loading at a certain displacement was made not different from the one attained in the shaking table test. The static loading was always controlled to a displacement rate of 0.2 cm/s.

## LOAD-DISPLACEMENT CHARACTERISTICS

### Monotonous Dynamic Loading Test

Fig.5 indicates load-displacement curves obtained from the monotonous dynamic loading tests. The initial stiffness, the yielding strength and the maximum strength under dynamic loads are considerably higher than those under static loads. In order to clarify these causes, the yielding strength and the maximum strength of the specimen under the monotonous dynamic loads were calculated using the stress-strain relationship of the steel bar considering the influence of strain rate effect shown in Fig.6, which shows the stress-strain curves of the steel bars obtained from dynamic tensile tests. The yield stress and the tensile strength increase remarkably with strain rate. In this case, the strength of concrete may also increase with loading rate. Since the longitudinal reinforcement ratio of the specimens used in this study is very small, however, the influence of the increase of the strength of concrete on the strength of the specimens is small. Therefore, only the stress-strain relationship of the steel bars due to strain rate effect was taken into account to calculate the strength of the specimens. The calculated values agree well with the observed ones, as indicated in Table.4. That is, the strength of R.C. members under the monotonous dynamic loads depends considerably on the loading rates, and it is possible to obtain the strength of R.C. members under the monotonous dynamic loads by considering the increase of the stress of the steel bars due to strain rate effect.

### Dynamic Cyclic Loading Test

In order to obtain the resisting force under dynamic cyclic loading at high loading rate, the horizontal inertia force described previously cannot be disregarded. Therefore, it is necessary to consider the influence of this horizontal inertia force using Equation (1).

$$P_t = P_{ot} - (W_1 + W_2 + W_3) \times \ddot{X}_t \text{ -----(1)}$$

in which  $P_t$ = resisting force acting on specimen at time  $t$ ;  $P_{ot}$ = force measured by load cell at time  $t$ ;  $W_1$ = mass of the equipment fixed at the top of specimen;  $W_2$ = mass of the equipment fixed in the exterior side of load cell at the top of actuator;  $W_3$ =(mass of the column) $\times$ 33/144;  $\ddot{X}_t$ = acceleration at the top of specimen at time  $t$ . The force given by Equation (1), that is  $P_t$ , is regarded as the dynamic load under the dynamic cyclic loading tests. Fig. 7 shows hysteresis curves obtained from the dynamic cyclic loading tests. These hysteresis curves are the ones at the first cycle of every displacement amplitude, and the loading rates are 0.1, 10, and 100 cm/s, respectively. Fig.8 shows skeleton curves obtained from these hysteresis curves. The hysteresis curves in the loading rates of 10 cm/s show almost the same shape as those in the loading rates of 0.1 cm/s, and the maximum strengths obtained from both curves also indicate almost the same values. In other words, the differences of the load-displacement curves are not recognized between the loading rates of 0.1 and 10 cm/s.

In regard to the load-displacement characteristics in the loading rates of 0.1 and 100 cm/s, the peak load of the hysteresis curves in 100 cm/s(DD-3) is about 20 % higher than that in 0.1 cm/s(DD-1) when the displacement is in the range of  $dy$  and  $2dy$  ( $dy$ :beam tip displacement when the steel bar attains

the yield strain). This reason is as follows; in the case of the loading rate of 100 cm/s, when the displacement passes the yield displacement and turns back at the first cycle, the strain of the steel bar at the root of the column increases from the elastic range into the plastic range, and at the moment when the strain of the bar passes the yield strain, some magnitude of strain rate is produced as shown in Fig.9, so that the yield stress increases according to the magnitude of strain rate at that moment, as described above. Consequently, the peak load of the hysteresis curve at the first cycle in 100 cm/s is higher than that in 0.1 cm/s when the displacement is in the range of  $dy$  and  $2dy$ . However, the differences in the peak loads after the second cycle between the loading rates of 0.1 and 100 cm/s are hardly recognized. This is because the strain of the steel bar after the second cycle does not follow the same stress-strain path as experienced at the first cycle, as shown in Fig.10.

When the displacement is larger than  $2 dy$ , both hysteresis curves become almost the same shape, and the peak loads obtained from both curves also indicate the same value. In other words, the influences of the loading rates under dynamic cyclic loading on the load-displacement characteristics in this range is considerably small as compared with those under monotonous dynamic loading. In order to clarify this cause, time history of the displacement and the strain of the bar was obtained from the results of the dynamic cyclic tests. As shown in Fig.11, the phase of the displacement almost coincide with that of the strain, so that the displacement rates and the strain rates at the turning point of the dynamic hysteresis curves become equally zero. For this reason, the influence of the loading rates under dynamic cyclic loading on the load-displacement characteristics is considerably small, except the case that the displacement exceeds the yield displacement and turns back at the turning point which is a little larger than the yield displacement in the hysteresis loop at the first cycle. At the same time, however, it should be pointed out that such a tendency that the load and the ductility decrease suddenly after the ultimate displacement ( $5-6dy$ ) was observed from the skeleton curves in the loading rate of 100 cm/s.

#### Shaking Table Test and Static Cyclic Test

The shaking table tests and static cyclic tests were carried out to confirm the results given by the dynamic cyclic tests. When such a single degree-of-freedom specimen as shown in Fig.1 is subjected to steady-state dynamic loading, the equation of dynamic equilibrium is

$$m\ddot{y} + f(y, \dot{y}; t) = -m\ddot{u} \quad \text{-----(2)}$$

in which  $y, \dot{y}, \ddot{y}$  = displacement, velocity and acceleration of the mass relative to the ground, respectively;  $m$  = mass;  $\ddot{u}$  = ground acceleration. The function  $f(y, \dot{y}; t)$  indicates the resisting force of the specimen, and generally this force is the one denoted as  $(c\dot{y} + ky)$ , in which  $c$  = viscous damping coefficient,  $k$  = elastic stiffness. In this study, the resisting force under shaking table tests, that is  $f(y, \dot{y}; t)$  or  $-m(\ddot{y} + \ddot{u})$ , is defined as the dynamic resisting force, and the hysteresis curve determined by the dynamic resisting force-displacement relationship is defined as the dynamic hysteresis curve.

Load-displacement characteristics obtained from static tests and shaking table tests are considerably influenced by the number of the repetition of loading. To eliminate this influence, the number of repetition of load at a certain displacement were made not different from each other, as described

previously. Fig.12 shows hysteresis curves obtained from both tests. As these curves are the ones at the first cycle of every displacement amplitude, they are not influenced by the number of the repetition of the loading at the same displacement amplitude. When the displacements at the top of the specimen are between  $\delta_y$  and  $3\delta_y$ , hysteresis curves obtained from the static tests show a slightly reversed-S shape while those obtained from the shaking table tests show a spindle shape. However, both hysteresis curves become almost the same shape in larger displacements ( $3\delta_y$ - $6\delta_y$ ). The influences of the loading rates on the load-displacement characteristics are considerably small as compared with those under dynamic cyclic loads of 100 cm/s. The reason for this may be that the maximum loading rate under the shaking table test is about 20 cm/s, which is much slower than 100 cm/s. Therefore, differences between the load-displacement characteristics under the shaking table tests and the static cyclic loading tests are hardly recognized even in the range of displacement shortly after the yielding one.

#### INFLUENCE OF LOADING RATE ON DAMPING

The damping of R.C. structures subjected to dynamic loading has not yet been completely clarified. A viscous damping, which is generally used, produces a damping force in proportion to velocity relative to the ground. If such a damping force occurs, the shape of the dynamic hysteresis loops and the magnitude of the force at the point where the maximum velocity can occur in a hysteresis loop must change depending on the magnitude of the loading rates.

Dynamic hysteresis loops shown in Fig.7 indicate almost the same shape regardless of the loading rates, and the shape of the hysteresis curves and the magnitude of the force at the point where the displacement is equal to zero or the maximum velocity occurs in each hysteresis curve are hardly influenced by the loading rates. This result shows that the viscous damping force hardly occurs.

#### CONCLUSIONS

In order to clarify the dynamic properties of R.C. piers, small single degree-of-freedom specimens, which have similar shapes to ordinary R.C. piers, were tested under static cyclic loading, dynamic loading and dynamic base motion. From the test results, it is concluded that;

- 1) The load-displacement curves obtained from the monotonous dynamic tests are considerably influenced by the loading rates. That is, the maximum strength increases remarkably with loading rate due to strain rate effect of steel bars.
- 2) The influence of the loading rates under dynamic cyclic loading on the load-displacement characteristics is considerably small as compared with that under monotonous dynamic loading because the displacement rates and the strain rates of the steel bar at the turning point of the dynamic cyclic hysteresis curves become equally zero. However, when the displacement turns back at the turning point which is a little larger than the yield displacement in the hysteresis loop at the first cycle, the peak load of that dynamic hysteresis curve becomes high due to strain rate effect.
- 3) Few differences in the shapes and the areas of the hysteresis curves due to the loading rate are recognized, except that hysteresis curves obtained from the static tests show a slightly reversed-S shape while the ones obtained from the shaking table tests show a spindle shape when the displacement at the

4) In the R.C. structures subjected to dynamic loading, the viscous damping force depending on velocity hardly occurs.

This research was supported by the Grant-in-aid for Scientific Research from Japanese Ministry of Education. A part of this study was conducted as the joint research by Saitama University and the Public Works Research Institute, Ministry of Construction, Japan.

- (1) Mutsuyoshi, H. and Machida, A. "Dynamic Properties of Reinforced Concrete Piers", Proceeding of the 6th Japan Earthquake Engineering Symposium, Dec. 1982
- (2) Sahara, T., Mutsuyoshi, H. and Machida, A., "Influence of Loading Rate on Behaviors of Reinforced Concrete Members", Preprint of the 38th Annual Meeting of JSCE, No. 5, pp. 369-370, Sep. 1983
- (3) Iwasaki, T., Hagiwara, R. and Koyama, T., "Dynamic Behavior of a Reinforced Concrete Bridge Pier Subjected to Cyclic Loadings", Proceeding of the 6th Japan Earthquake Engineering Symposium, Dec. 1982

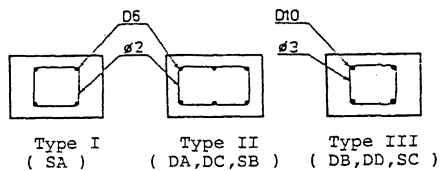
| Specimen | Tensile Reinf. Ratio (%) | Shear Reinf. Ratio (%) | Loading Method | Loading Rate (cm/s) |  |
|----------|--------------------------|------------------------|----------------|---------------------|--|
| DA-1     | 0.8                      | 0.1                    | Monotonic      | 0.1                 |  |
| DA-2     |                          |                        |                | 100.0               |  |
| DB-1     | 1.18                     | 0.09                   |                | 0.1                 |  |
| DB-2     |                          |                        |                | 100.0               |  |
| DC-1     | 0.8                      | 0.1                    | Cyclic         | 0.1                 |  |
| DC-2     |                          |                        |                | 10.0                |  |
| DC-3     |                          |                        |                | 100.0               |  |
| DD-1     |                          |                        |                | 0.1                 |  |
| DD-2     | 1.18                     | 0.09                   |                | 10.0                |  |
| DD-3     |                          |                        |                | 100.0               |  |

| Specimen | Tensile Reinf. Ratio (%) |      | Spacing of Stirrups (cm) | Shear Reinf. Ratio (%) | Number of Cycles | Loading Method | Failure Mode |
|----------|--------------------------|------|--------------------------|------------------------|------------------|----------------|--------------|
| SA-1     | 2D6                      | 0.53 | Ø2-8                     | 0.05                   | 64               | D              | Flexure      |
| SA-2     |                          |      | Ø2-4                     | 0.1                    | 105              | S, D           |              |
| SB-1     | 3D6                      | 0.79 | Ø2-8                     | 0.05                   | 169              | S, D           |              |
| SB-2     |                          |      | Ø2-4                     | 0.1                    | 237              | S, D           |              |
| SB-3     |                          |      | Ø2-3                     | 0.14                   | 565              | S, D           |              |
| SC-1     | 2D10                     | 1.18 | Ø3-20                    | 0.05                   | 481              | S, D           | Shear        |
| SC-2     |                          |      | Ø3-10                    | 0.09                   | 1002             | S, D           |              |
| SC-3     |                          |      | Ø3-8                     | 0.12                   | 1205             | D              | Flexure      |

Technical drawings of three types of reinforced concrete columns:

- Type I, III:** Square column with a width of 400 mm and a height of 600 mm. The base is 400 mm wide. Reinforcement details show a top section with dimensions 100, 20, 60, 20, 20, and 20. A load  $P$  is applied at the top.
- Type II:** Rectangular column with a width of 300 mm and a height of 600 mm. The base is 400 mm wide. Reinforcement details show a top section with dimensions 150, 20, 55, 20, 20, and 20.

Dimensions are in mm.



918

Table 3 Frequency for dynamic cyclic tests  
(Hz) (DC-1,2,3)

| Displacement<br>(cm)   | —    | $\delta y$ | $2\delta y$ | $3\delta y$ | $4\delta y$ | $5\delta y$ | $6\delta y$ | $7\delta y$ |
|------------------------|------|------------|-------------|-------------|-------------|-------------|-------------|-------------|
| Loading<br>Rate (cm/s) | 0.2  | 0.7        | 1.4         | 2.1         | 2.8         | 3.5         | 4.2         | 4.9         |
| 0.1                    | 0.08 | 0.023      | 0.011       | 0.008       | 0.006       | 0.005       | 0.004       | 0.003       |
| 10.0                   | 8.0  | 2.3        | 1.1         | 0.8         | 0.6         | 0.5         | 0.4         | 0.3         |
| 100.0                  | 30.0 | 22.7       | 11.4        | 7.6         | 5.7         | 4.5         | 3.8         | 3.2         |

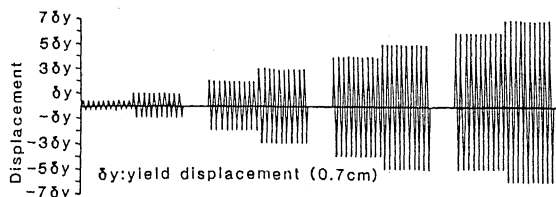
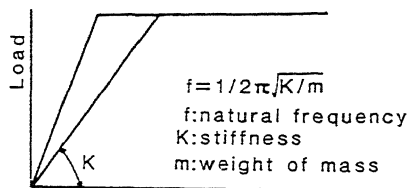


Fig.2 Loading program

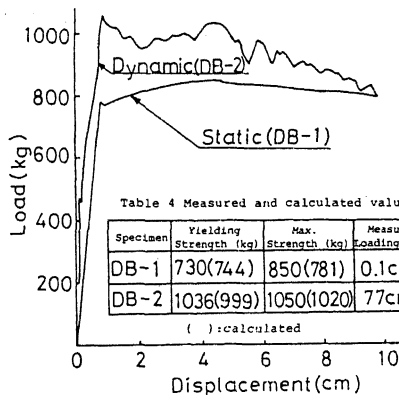


Fig.5 Load-displacement relationship obtained from monotonous dynamic loading test

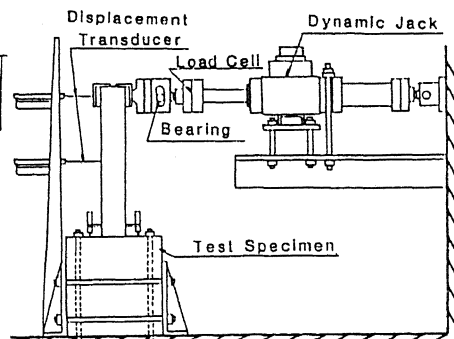


Fig.3 Loading system for dynamic test

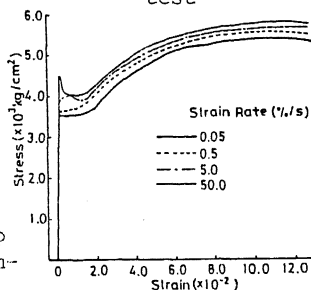


Fig.6 Stress-strain relationship obtained from dynamic tensile test of steel bar (SD30,D10) (Ref.2)

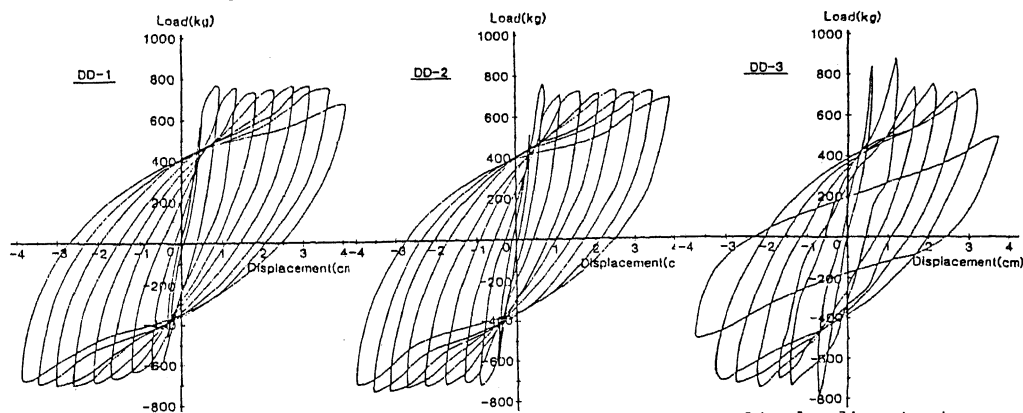


Fig.7 Hysteresis curves obtained from dynamic cyclic loading test

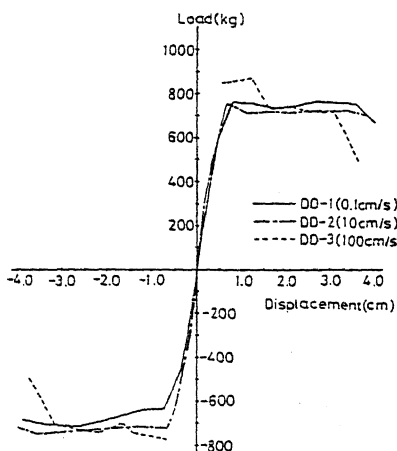


Fig.8 Skeleton curves obtained from dynamic cyclic test

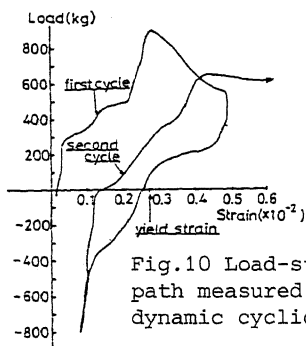


Fig.10 Load-strain path measured from dynamic cyclic test

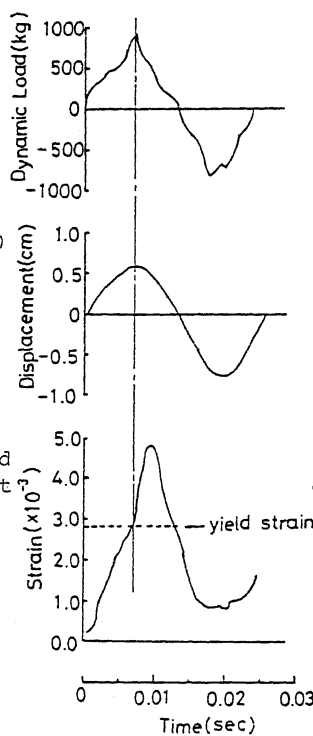


Fig.9 Time history of dynamic load, displacement and strain of steel bar at first cycle

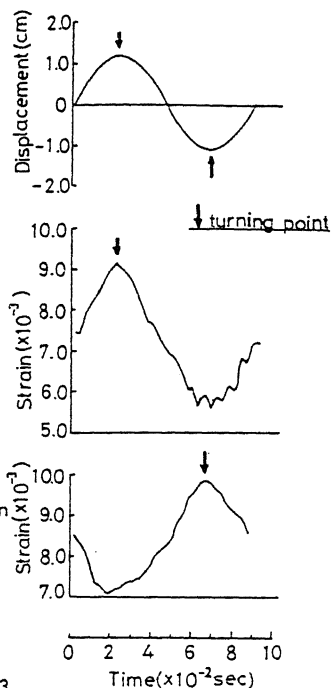


Fig.11 Time history of displacement and strain after second cycle

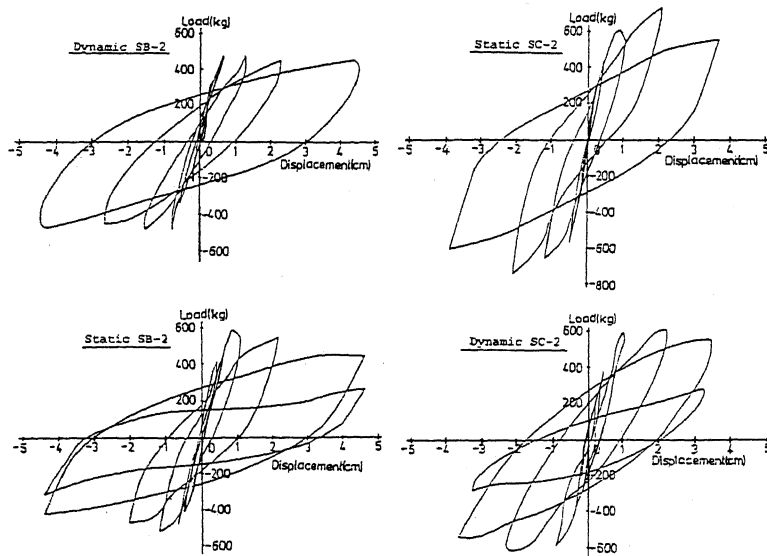


Fig.12 Hysteresis curves obtained from shaking table tests ( $\Delta y=0.7\text{cm}$ )